On the Influence of the Antenna Pattern in Noncoherent Massive MIMO Systems

George Yammine[1], Robert F.H. Fischer[1], Christian Waldschmidt[2]
[1]Institut für Nachrichtentechnik, [2]Institut für Mikrowellentechnik
Universität Ulm, Ulm, Germany
Email: {george.yammine, robert.fischer, christian.waldschmidt}@uni-ulm.de

***Abstract*—Noncoherent multi-user detection schemes are attractive in multi-user massive MIMO uplink systems. In particular, sorted decision-feedback differential detection (DFDD) in combination with noncoherent decision-feedback equalization (nDFE) over the users has been shown to perform well though avoids the need for channel estimation. Up to now, in all studies a uniform linear receiver array employing omni-directional antennas has been assumed. In this paper, we assess the influence of the antennas' radiation patterns on the performance of the noncoherent massive MIMO. Based on analytic expressions, we present an optimization approach for the array assuming that the individual antennas are electronically switchable to change the direction of the main radiation. The gains are assessed by means of numerical simulations. It is shown that in the noncoherent setting the antenna pattern has a much more pronounced influence and, thus, has to be designed more carefully than in the coherent case.**

I. Introduction

Multiple-input/multiple-output (MIMO) systems, where the base station is equipped with a very large number of receive antennas, so-called *massive MIMO* systems, gain more and more attention, e.g., [8], [9]. The drawback of massive MIMO is that the estimation of a huge number of channel coefficients is required, which quickly becomes challenging.

One way to eliminate the need for channel estimation in a multi-user massive MIMO uplink system is to resort to *noncoherent detection*. Exploiting the similarities between ultra-wideband (UWB) systems [10] and massive MIMO, noncoherent detection schemes were presented in [11], [6] and assessed for a uniform linear array with omni-directional antennas. If the users are sufficiently spatially separated, the performance of these schemes is comparable to coherent detection with non-perfect channel knowledge. However, in contrast to coherent schemes where phase information is utilized, the performance degrades if the users are close to each other.

In this paper, we analyze the influence of the antenna pattern on the performance of noncoherent massive MIMO systems. To this end, we employ idealized antenna patterns which, however, reflect that of physically realizable ones [2], [13]. Having gained an insight into the impact of the antenna pattern, based on an analytic expression of the signal-to-interference-plus-noise ratio (SINR), we present an optimization approach for the array assuming that the individually antennas are (electronically) controllable. The gains are assessed by means of numerical simulations.

978-1-4673-6540-6/15/$31.00

The paper is organized as follows. In Sec. II, the system model and the antenna patterns are introduced and noncoherent multi-user detection in massive MIMO is briefly reviewed. Numerical results are presented and discussed in Sec. III. The optimization of the antenna array is given and evaluated in Sec. IV. Conclusions are drawn in Sec. V.

II. System Model and Noncoherent Detection

We consider a *multi-user uplink scenario* where N_u users with a single (omni-directional) antenna simultaneously transmit to a central receiver equipped with $N_\mathsf{rx} \gg 1$ antennas, illustrated in Fig. 1. In each time step k, user u transmits an M-ary differentially encoded PSK symbol $b_{k,u}$ drawn from $\mathcal{M} \overset{\text{def}}{=} \{\mathrm{e}^{\mathrm{j}2\pi \cdot i/M} \mid i = 0, 1, \ldots, M-1\}$. In the receiver, noncoherent detection methods are applied, cf. Sec. II-C.

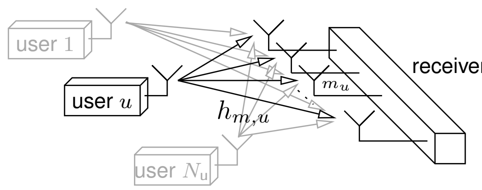

Fig. 1. Multi-user massive MIMO uplink system.

A. Geometric System Model

As in [11], a uniform linear array (antenna spacing d_a) is assumed at the receiver. The N_u users are located in front of the array; user u at a distance d_u and position m_u, cf. Fig. 2. The model in [11], which assumed omni-directional (isotropic) antennas, is now generalized to include the effect of different antenna radiation patterns.

The discrete-time model (symbol interval T; equivalent complex baseband) of the individual channels between user u and antenna element m comprise pulse shaping at the transmitter, the continuous-time flat-fading channel (with attenuation, path loss, and fast fading), matched filtering, and symbol-spaced sampling at the receiver. The channel coefficient $h_{m,u}$ is hence given as

$$h_{m,u} = c_\mathrm{h} \cdot r_{m,u}^{-\gamma/2} \cdot C(\psi_{m,u}) \cdot h_{u,b,\mathrm{i.i.d.}} \,. \qquad (1)$$

Here, $r_{m,u}^{-\gamma/2}$ is the component due to the path loss (distance $r_{m,u}$ and *path loss exponent* γ), $C(\psi_{m,u})$ models the antenna pattern (w.r.t. voltage on a linear scale), where $\psi_{m,u}$ is the relative angle (cf. Fig. 2) between antenna m and user u. The i.i.d. zero-mean unit-variance complex Gaussian random variable $h_{m,u,\text{i.i.d.}}$ accounts for fast fading effects which are caused by scatterers located in vicinity of the user; c_h is a normalization constant.

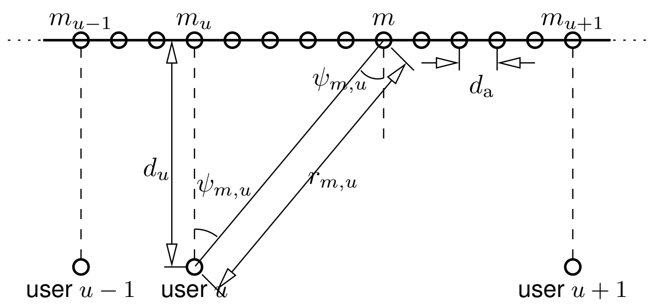

Fig. 2. Geometric system model for multi-user massive MIMO transmission.

The model can be specified via the average received power $P_{m,u}$ at each antenna m induced by user u, i.e., the *power-space profile (PSP)* [11]. Since $h_{m,u}$ is zero-mean, this calculates to (cf. [11])

$$\begin{aligned} P_{m,u} &\stackrel{\text{def}}{=} \mathrm{E}\{|h_{m,u}|^2\} \quad (2)\\ &= \mathrm{E}\{|c_\text{h} \cdot r_{m,u}^{-\gamma/2} \cdot C(\psi_{m,u}) \cdot h_{u,b,\text{i.i.d.}}|^2\} \\ &= c_\text{p} \cdot \mathrm{e}^{-\gamma/2 \cdot \log(1+|m-m_u|^2/d_{\text{r},u}^2)} \cdot |C(\psi_{m,u})|^2 \\ &\approx c_\text{p} \cdot \mathrm{e}^{-|m-m_u|^2/(2\zeta^2)} \cdot |C(\psi_{m,u})|^2 \;, \quad (3) \end{aligned}$$

where $d_{\text{r},u} \stackrel{\text{def}}{=} d_u/d_\text{a}$ is the relative distance (normalized to the antenna spacing) of the user u to the array; m_u and $d_{\text{r},u}$ characterize the user; $c_\text{p} = |c_\text{h}|^2$ is a normalization constant. The quotient $\zeta^2 \stackrel{\text{def}}{=} d_{\text{r},u}^2/\gamma$ is then used to describe the path loss in relation to the relative distance of the user u. From Fig. 2, the angle $\psi_{m,u}$ under which user u is seen by antenna m, calculates to

$$\psi_{m,u} = \tan^{-1}(|m-m_u|, d_{\text{r},u}) \;, \quad (4)$$

using the 2-argument arc-tangent function, $\tan^{-1}(y,x)$.

B. Idealized Antenna Patterns

In order to reduce the overlap in the PSP of neighboring users and hence achieve a better user separation, the antenna pattern should have some directed characteristics. In the present study, an idealized antenna with pattern [2], [13]

$$C(\psi) = \sqrt{G_\text{i}}\cos(\psi \cdot N_\mathsf{notch}/2) \quad (5)$$

is assumed, where $N_\mathsf{notch} \in \mathbb{N}$ is the number of notches or nulls in the pattern. The boresight of each individual antenna, $\psi = 0°$, is always perpendicular to the array; all boresights are parallel to each other. The boresight gain G_i is chosen such that the average received power seen by the antennas in the array is that of an omni-directional (isotropic) antenna, i.e.,

$$\frac{1}{2\pi}\int_{-\pi}^{\pi} |C(\psi)|^2 \, \mathrm{d}\psi = 1 \;. \quad (6)$$

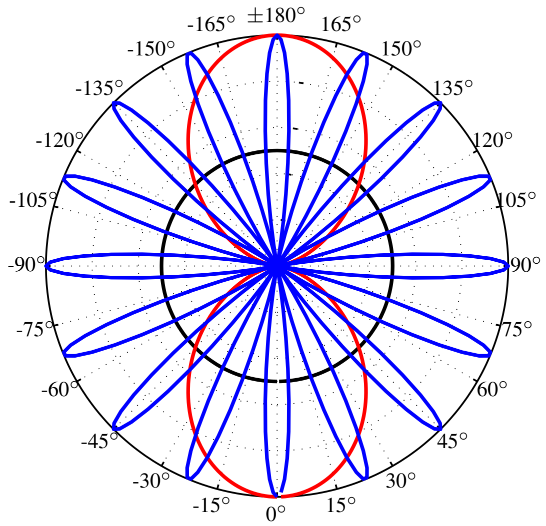

Fig. 3. Azimuth gain plot, i.e., $G(\psi)$ versus the azimuth angle ψ. Black: omni-directional ($N_\mathsf{notch} = 0$); Red: $N_\mathsf{notch} = 2$; Blue: $N_\mathsf{notch} = 16$.

Fulfilling (6), we have $G_\text{i} = 2$, and we can define the *antenna gain pattern* (w.r.t. power) as

$$G(\psi) \stackrel{\text{def}}{=} |C(\psi)|^2 \;, \quad (7)$$

and set $G(\psi) = 1$ for $N_\mathsf{notch} = 0$, i.e., for an omni-directional antenna.

An example of antennas with different gain patterns can be seen in Fig. 3.

C. Noncoherent Detection

We assume a block fading channel model, where the fading coefficients $h_{m,u}$ are randomly chosen according to (1) but then constant over a burst of size N_bl. In view of block-wise processing applying *multiple-symbol differential detection (MSDD)* [4] or its reduced-complexity version *decision-feedback differential detection (DFDD)* [1], [12], we consider the receive block over the N_rx receive antennas and over N_bl time steps. It is given by [11]

$$\boldsymbol{R} = \sum_{u=1}^{N_\text{u}} \boldsymbol{h}_u \boldsymbol{b}_u + \boldsymbol{N} \;, \quad (8)$$

where $\boldsymbol{h}_u \stackrel{\text{def}}{=} [h_{1,u}, \ldots, h_{N_\mathsf{rx},u}]^\mathsf{T}$ is the (column) vector of channel coefficients for user u and $\boldsymbol{b}_u \stackrel{\text{def}}{=} [b_{0,u}, \ldots, b_{N_\mathsf{bl}-1,u}]$ is the (row) vector of transmit symbols of user u. The matrix $\boldsymbol{N}$ collects the circular-symmetric zero-mean complex Gaussian noise $n_{m,k}$ with variance σ_n^2.

Differential detection of the symbols of user u can then be based on the $N_\mathsf{bl} \times N_\mathsf{bl}$ *correlation matrix*

$$\boldsymbol{Z}_u \stackrel{\text{def}}{=} \boldsymbol{R}^\mathsf{H} \boldsymbol{W}_u \boldsymbol{R} \;, \quad (9)$$

using the user-specific diagonal weighting matrix [11]

$$\boldsymbol{W}_u \stackrel{\text{def}}{=} \mathbf{diag}(w_{1,u}, \ldots, w_{N_\mathsf{rx},u}) \;. \quad (10)$$

The operation of DFDD in the massive MIMO scenario was given in [11]. Performance improvements can be obtained by additionally applying *noncoherent decision-feedback equalization (nDFE)* over the users [6]. DFDD/nDFE establishes a low-complexity but well-performing strategy for noncoherent multi-user detection. A sufficiently accurate approximation of the *signal-to-noise-plus-interference (SINR)* for DFDD/nDFE was derived in [6]. For user u it reads

$$\mathrm{SINR}_u = \frac{\eta_{u,u}^2 + \sigma_{u,u,u}^2}{\sum\limits_{\nu\notin\mathcal{D},\nu\neq u} \eta_{u,\nu}^2 + \sum\limits_{(\nu,\mu)\neq(u,u)} \sigma_{u,\nu,\mu}^2 + \sigma_{\mathrm{n},u}^2} , \quad (11)$$

where $\mathcal{D}$ is the index set of the already detected users and

$$\eta_{u,\nu} \stackrel{\text{def}}{=} \sum\nolimits_{m=1}^{N_{\mathsf{rx}}} w_{m,u} P_{m,\nu} , \quad (12)$$

$$\sigma_{u,\nu,\mu}^2 \stackrel{\text{def}}{=} \sum\nolimits_{m=1}^{N_{\mathsf{rx}}} w_{m,u}^2 P_{m,\nu} P_{m,\mu} , \quad (13)$$

$$\sigma_{\mathrm{n},u}^2 \stackrel{\text{def}}{=} \sum\nolimits_{m=1}^{N_{\mathsf{rx}}} w_{m,u}^2 \big(\sigma_{\mathsf{n}}^4 + 2\sigma_{\mathsf{n}}^2 \sum\nolimits_{\nu=1}^{N_{\mathsf{u}}} P_{m,\nu}\big) . \quad (14)$$

A close look reveals that the SINR purely depends on the PSP $P_{m,u}$ and the weighting factors $w_{m,u}$, $u = 1,\dots,N_{\mathsf{u}}$, $m = 1,\dots,N_{\mathsf{rx}}$ (we assume the noise variance σ_{n}^2 is also known). Hence, given the PSP, the weighting factors can be adjusted in order to maximize the SINR of each user individually. In this paper, this is done via numerical optimization. The use of a Gaussian weighting with optimized window width as in [11], [6] is no longer suited in the present case of multi-modal PSPs.

III. Simulation Results

Simulations were conducted for a $N_{\mathsf{u}} = 3$ user scenario, as depicted in Fig. 2, using a $N_{\mathsf{rx}} = 100$ antenna uniform linear array. Users 1 (■) and 3 (■) are placed in front of antennas 20 and 85, respectively. The position of user 2 (■) is varied between antenna 30 and 70. A relative distance $d_{\mathrm{r},u} = 38$ and propagation exponent $\gamma = 3.6$ were chosen (resulting in $\zeta_u = 20$, $\forall u$, as in [11]). The PSPs are calculated according to (3) and the PSP of each user is normalized (constant c_{p}) for an average total receiver power of one. This guarantees a comparison purely based on the interference situation / shape of the PSP and eliminates effects of different scalings. The noise power is fixed such that $E_{\mathsf{s}}/N_0 = 1/\sigma_{\mathsf{n}}^2 \mathrel{\hat=} 14$ dB.

Each user transmits differentially encoded 4PSK symbols; the block length is $N_{\mathsf{bl}} = 200$. Detection is either performed via DFDD (individually per user) or DFDD with noncoherent DFE over the users (DFDD/nDFE with optimal detection order). In each case, the required weighting factors are adjusted via numerical optimization using Matlab's nonlinear optimization tools.[1]

For comparison, coherent BLAST [7] with *perfect channel knowledge* is included in the numerical simulation results. In Fig. 4, the symbol error rate is depicted over the the position m_2 of user 2. Colors correspond to users. From left to right and first/second row the results for omni-directional antennas ($N_{\mathsf{notch}} = 0$), $N_{\mathsf{notch}} = 2$, 4, 8, 16, and 32 are shown. Please note that the entire array always uses the same antenna type.

As already observed in [6], when user 2 is close to user 1 or 3, a degradation in the performance of said users is present since there is a high overlap of the users' PSPs. This degradation is differently pronounced for the antenna types. Worst case are clearly omni-directional antennas. Using $N_{\mathsf{notch}} = 2$, the main lobe width seen by the transmitting users is approximately that of the omni-directional antenna, and, hence, performance is similar to $N_{\mathsf{notch}} = 0$. Good results are achieved with $N_{\mathsf{notch}} = 4$; here a strong directivity perpendicular to the array is present; little interference is caused by the other users. For $N_{\mathsf{notch}} \geq 8$ a fluctuation of the performance over the position is visible. This is due to the interference collected by the side lobes of the antenna pattern.

If significant interference (especially for the middle user (■)) is present, employing nDFE will provide substantial gains. If interference is largely avoided by the antenna design (as for $N_{\mathsf{notch}} = 4$), only little can be gained. We can also note that in contrast to using the Gaussian weighting with optimized window width only as in [11], [6], the performance of DFDD and DFDD/nDFE is (almost) the same for users 1 (■) and 3 (■) when numerically optimizing the weighting factors. Using the optimized weighting factors almost all interference from user 3 (■) into user 1 (■) is avoided (and vice versa), and no further cancellation of (average) interference is required.

A comparison with the BLAST scheme reveals two observations. First, as a well-known fact, there is a performance loss of the noncoherent scheme compared to the coherent one. However, this comparison is not really fair, as perfect channel knowledge is assumed. Taking the estimation error, obtained with practical finite-length training, and the rate loss due to the necessity of accommodating the training symbols in the burst into account, the noncoherent scheme may even outperform the coherent one, cf., e.g., [5].

Second, as can be seen from Fig. 4, in the coherent case, the performance of the users is independent of the position. This is due to the fact that here the *phases* of the channel coefficients can be utilized. Via this phase information, even closely spaced user can be separated. Moreover, the performance of BLAST is almost independent of the used antenna pattern.[2]

In summary, it can be stated that when using noncoherent detection, the antenna pattern has a much more significant influence on the performance. In a practical situation, coherent detection—with the need of pilot symbols and channel estimation—and noncoherent schemes can, in principle, have a similar performance. The strong influence of the PSP on the performance of noncoherent schemes can be used to optimize the antenna patterns in a given scenario.

[1]For the numerical simulations, the positions of the three users—which are required for the optimization of the weighting factors—are assumed to be perfectly known. This assumption is valid, since the user position can be accurately estimated by means of eigenvalue decomposition of the receive matrix $\boldsymbol{R}$. Additionally, since the antenna configuration is known at the receiver, the PSP can be estimated with sufficient accuracy from $\boldsymbol{R}$.

[2]The slight differences in the performance can be explained as follows: According to the PSP, a certain number of antennas receive significant power and hence is "relevant" for a user. Since in the varying scenarios and for the individual users a different number of antennas is relevant, i.e., a different number of channel coefficients are active, the receiver-side combining leads to different diversity orders. Noteworthy, as the receiver power is normalized, the slightly different performance of the users is not due to varying powers.

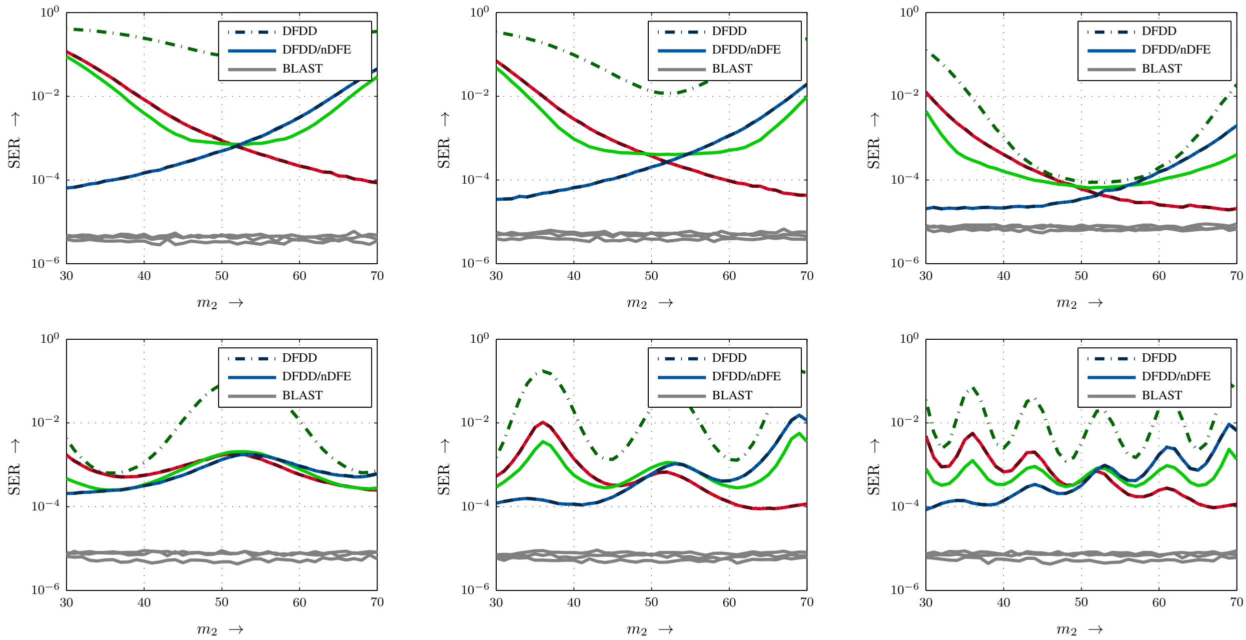

Fig. 4. Symbol error rate vs. the position of user 2 (■) using different antenna patters. Top row: omni-directional, $N_{\text{notch}} = 2$, $N_{\text{notch}} = 4$; bottom row: $N_{\text{notch}} = 8$, $N_{\text{notch}} = 16$; $N_{\text{notch}} = 32$. $E_s/N_0 \mathrel{\widehat{=}} 14$ dB. $N_u = 3$; $m_1 = 20$ (■), $m_3 = 85$ (■); colors corresponding to users; grayed colors: BLAST. Uniform linear array with $N_{\text{rx}} = 100$ antenna elements. Power-space profile according to (3) with $d_{r,u} = 38$ and $\gamma = 3.6$, $\forall u$, and normalized to unit power per user. Burst length $N_{\text{bl}} = 200$. $M = 4$-ary DPSK.

IV. Optimization of the Antenna Pattern

As seen in the last section, the antenna pattern has a significant influence on the performance. Consequently, we introduce new degrees of freedom to optimize the antenna pattern/antenna configuration to achieve best performance in the noncoherent case.

A suited criterion for optimization is the minimum SINR of the users. Since the receive weighting has to be optimized individually for each user, we have

$$\text{minSINR} \overset{\text{def}}{=} \min_{u=1,\ldots,N_u} \Big(\max_{\substack{w_{m,u} \\ m=1,\ldots,N_{\text{rx}}}} \text{SINR}_u \Big) . \tag{15}$$

Consequently, by choosing the radiation pattern $G_m(\psi)$ of antenna m, we change the PSP (3) and hence can optimize the minimum SINR. Assuming we have N_A different antenna patterns which are collected in the set $\mathcal{G} \overset{\text{def}}{=} \{G^{(1)}(\psi),\ G^{(2)}(\psi),\ \ldots,\ G^{(N_A)}(\psi)\}$, the optimization task reads

$$\{G_1, \ldots, G_{N_{\text{rx}}}\} \overset{\text{def}}{=} \operatorname*{argmax}_{\substack{G_m \in \mathcal{G} \\ m=1,\ldots,N_{\text{rx}}}} \text{minSINR} . \tag{16}$$

For this optimization, a greedy approach is employed. The optimization algorithm is given in the pseudo-code as Alg. 1. The algorithm (which returns the vector $\boldsymbol{a} = [a_1, \ldots, a_{N_{\text{rx}}}]$ of pattern numbers) iterates over all antennas, selecting the radiation pattern $G_m^{(a)}(\psi)$, $a = 1, \ldots, N_A$, $m = 1, \cdots, N_{\text{rx}}$, which locally maximizes the minimum SINR.

A. Using Electronically Switchable Antennas

One possible degree of freedom for optimization is to employ electronically switchable antennas [3], where the boresight lobe can be switched between two different angles. A simple and natural choice is to use a rotation angle of $\frac{\pi}{N_{\text{notch}}}$; here main lobes and notches are simply interchanged. Hence using (5) and (7), we have $G^{(1)}(\psi) = G(\psi)$ and $G^{(2)}(\psi) = G(\psi + \pi/N_{\text{notch}})$.

Algorithm 1 Pseudo-code representation of antenna optimization algorithm for massive MIMO.

$\boldsymbol{a} = \texttt{optAntennas}(\mathcal{G},\ N_{\text{rx}},\ N_{\text{iter}})$

$\boldsymbol{a} = [a_m]$, $a_m := 0$, $m = 1, \ldots, N_{\text{rx}}$
`for` $l = 1$ `to` N_{iter} {
  $\mathcal{D} := \texttt{randperm}(N_{\text{rx}})$
  `for` $\tilde{m} = 1$ `to` N_{rx} {
    calculate $P_{m,u}^{(a)}$ acc. to (3), using $G_{\mathcal{D}_{\tilde{m}}}^{(a)}$, $a = 1, \ldots, N_A$
    calculate $\text{minSINR}^{(a)}$ acc. to (15), $a = 1, \ldots, N_A$
    $a_{\mathcal{D}_{\tilde{m}}} = \text{argmax}_{a=1,\ldots,N_A} \text{SINR}^{(a)}$
  }
}
return $\boldsymbol{a}$

Numerical results for the $N_{\text{notch}} = 4$ scenario and two rotation angles are plotted in Fig. 5. Compared to the results of Fig. 4, we can see a more “balanced” performance of all 3 users. The best performing user, user 3 (■) when $m_2 \le 45$ and user 1 (■) when $m_2 \ge 55$ respectively, suffers a small performance loss, while the remaining users have a noticeable gain. This ensures a low error rate for all 3 users, rather independent of the position of user 2 (■). Additionally, we see that if the 3 users were sufficiently spatially separated, i.e., $45 \le m_2 \le 60$, interference is largely avoided; no further gains are achieved via nDFE.

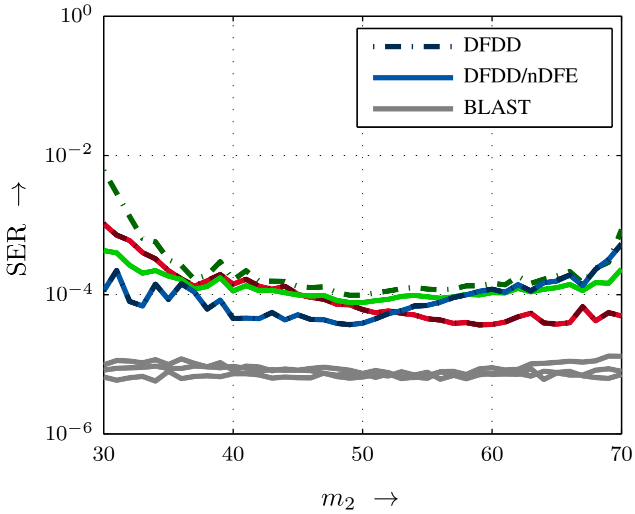

Fig. 5. Symbol error rate vs. the position of user 2 (■) using electronically switchable antennas with $N_{\mathsf{notch}} = 4$ and two rotation angles. $E_{\mathsf{s}}/N_0 \mathrel{\widehat{=}} 14$ dB. $N_{\mathsf{u}} = 3$; $m_1 = 20$ (■), $m_3 = 85$ (■); colors corresponding to users; grayed colors: BLAST. Uniform linear array with $N_{\mathsf{rx}} = 100$ antenna elements. Power-space profile according to (3) with $d_{\mathrm{r},u} = 38$ and $\gamma = 3.6$, $\forall u$, and normalized to unit power per user. Burst length $N_{\mathsf{bl}} = 200$. $M = 4$-ary DPSK.

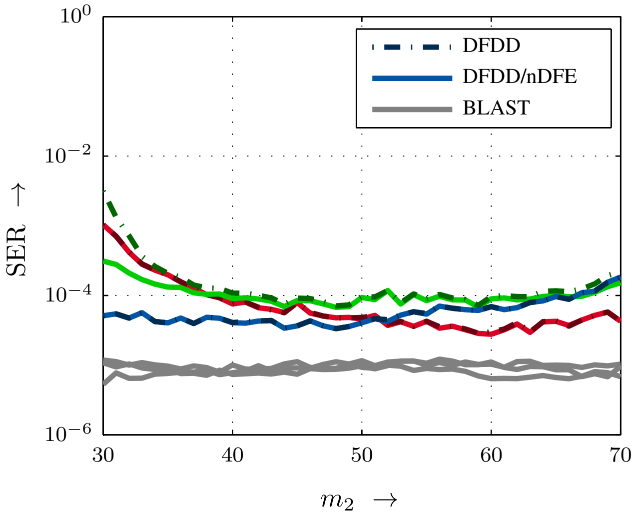

Fig. 6. Symbol error rate vs. the position of user 2 (■) using antennas where between $N_{\mathsf{notch}} = 4$ and $N_{\mathsf{notch}} = 8$ can be switched. $E_{\mathsf{s}}/N_0 \mathrel{\widehat{=}} 14$ dB. $N_{\mathsf{u}} = 3$; $m_1 = 20$ (■), $m_3 = 85$ (■); colors corresponding to users; grayed colors: BLAST. Uniform linear array with $N_{\mathsf{rx}} = 100$ antenna elements. Power-space profile according to (3) with $d_{\mathrm{r},u} = 38$ and $\gamma = 3.6$, $\forall u$, and normalized to unit power per user. Burst length $N_{\mathsf{bl}} = 200$. $M = 4$-ary DPSK.

B. Using Tuneable Antennas

A second approach to increase the spatial separation of the users is to have antennas in the array where between multiple radiation patterns can be switched, e.g., by means of radiation pattern tuning [14].

Numerical results for antennas where between $N_{\mathsf{notch}} = 4$ and $N_{\mathsf{notch}} = 8$ can be switched are plotted in Fig. 6. In both cases the angle of main radiation is $0°$. Compared to the results of Fig. 4, we see again the more "balanced" performance of all 3 users. With this configuration, almost the same results as in Fig. 5 for the case of rotation are obtained.

V. Conclusions

We have shown that, by using antennas with different radiation patterns, the performance of noncoherent multi-user massive MIMO systems can be influenced and significant performance gains can be achieved. This design can be used to reduce the SER over a larger range of positions. By using tuneable antennas that can generate different radiation patterns, an optimum performance scenario can be created to maximize the minimum SINR for all users. We have also shown that, by employing electronically switchable antennas in the array, and steering each individual antenna, or by employing antennas that can be tuned to different gain patterns, additional performance gain can be achieved which provides better quality of service for all users.

References

[1] F. Adachi, M. Sawahashi. Decision-Feedback Multiple-Symbol Differential Detection for Mary DPSK. *Electronics Letters*, pp. 1385–1387, July 1993.

[2] C.A. Balanis. *Antenna Theory: Analysis and Design*. Hoboken, NJ, Wiley Interscience, 2005.

[3] J. Chiao, Y. Fu, I. Chio, M. DeLisio, L. Lin. MEMS reconfigurable Vee Antenna. *Proceedings of IEEE MTT-S Microwave Symposium Digest*, vol. 4, pp. 1515–1518, June 1999.

[4] D. Divsalar, M.K. Simon. Multiple-Symbol Differential Detection of MPSK. *IEEE Tran. Communications*, pp. 300–308, Mar. 1990.

[5] R.F.H. Fischer, M. Bense, C. Stierstorfer. Noncoherent Joint Decision-Feedback Detection in Multi-User Massive MIMO Systems. In *Proceedings of International ITG/IEEE Workshop on Smart Antennas*, Erlangen, Germany, Mar. 2014.

[6] R.F.H. Fischer, M. Bense. Noncoherent Decision-Feedback Equalization in Massive MIMO Systems. In *Proceedings of International Zurich Seminar (IZS)*, pp. 112–115, Zurich, Switzerland, Feb. 2014.

[7] G.J. Foschini, D. Chizhik, M.J. Gans, C.Papadias, R.A. Valenzuela. Analysis and Performance of Some Basic Space-Time Architectures. *IEEE J. Sel. Areas in Communications*, pp. 303–320, Apr. 2003.

[8] T.L. Marzetta. Noncooperative Cellular Wireless with Unlimited Numbers of Base Station Antennas. *IEEE Trans. Wireless Communications*, pp. 3590–3600, Nov. 2010.

[9] F. Rusek, D. Persson, B.K. Lau, E.G. Larsson, T.L. Marzetta, O. Edfors, F. Tufvesson. Scaling Up MIMO: Opportunities and Challenges with Very Large Arrays. *IEEE Signal Processing Magazine*, pp. 40–60, Jan. 2013.

[10] A. Schenk. *Coding, Modulation, and Detection in Impulse-Radio Ultra-Wideband Communications*, PhD Thesis. University Erlangen-Nürnberg, 2012.

[11] A. Schenk, R.F.H. Fischer. Noncoherent Detection in Massive MIMO Systems. In *Proceedings of International ITG/IEEE Workshop on Smart Antennas*, Stuttgart, Germany, Mar. 2013.

[12] R. Schober, W.H. Gerstacker, J.B. Huber. Decision-Feedback Differential Detection of MDPSK for Flat Rayleigh Fading Channels. *IEEE Trans. Communications*, pp. 1025–1035, July 1999.

[13] S. Silver *Microwave Antenna Theory and Design*. Institution of Electrical Engineers, London, UK, 1984.

[14] Y. Tawk, C.G. Christodoulou, J. Costantine, S.E. Barbin. A Frequency and Radiation Pattern Reconfigurable Antenna System with Sensing Capabilities for Cognitive Radio. In *Proceedings of IEEE Antennas and Propagation Society International Symposium (APSURSI)*, Chicago, IL, USA, July 2012.